



Spatialization through a rainfall and evapotranspiration data mesh in the Pirapó River sub-basin using remote sensing

Lucas Vinicius Dias

Mestre, UEM, Brasil.
vinicioslukas_dias@hotmail.com

Lais Ferrer Amorim de Oliveira

Pesquisadora Doutora, USP, Brasil.
laisamorim@alumni.usp.br

Paulo Fernando Soares

Professor Doutor, UEM, Brasil.
psoares@uem.br

Cláudia Telles Benatti

Professora Doutora, UEM, Brasil.
ctbenatti@uem.br

Received: October 22, 2024

Accepted: November 5, 2024

Online Published: December 14, 2024

DOI: 10.17271/1980082720420245195

<https://doi.org/10.17271/1980082720420245195>

License

Copyright (c) 2024 Electronic Journal Fórum Ambiental da Alta Paulista



This work is licensed under a [Creative Commons Attribution 4.0 International License](https://creativecommons.org/licenses/by/4.0/)

Espacialização por meio de malha de dados de precipitação e evapotranspiração em sub-bacia do rio Pirapó utilizando sensoriamento remotos

RESUMO

O presente trabalho tem como objetivo utilizar dados de sensoriamento remoto dos produtos IMERG e GLDAS a partir de um grid de precipitação e evapotranspiração mensal médio para gerar uma análise espacializada das variáveis de precipitação e evapotranspiração na sub-bacia do Rio Pirapó, com exultório na estação de captação de água de Maringá, Paraná, visando a melhoria no monitoramento e gestão dos recursos hídricos. Foi aplicada uma abordagem quantitativa com o uso de uma malha de 07x09 células (100 km² por célula) para mapear as variáveis ambientais de 2000 a 2020. A precipitação foi analisada utilizando polígonos de Thiessen com dados de cinco estações pluviométricas e a evapotranspiração foi obtida por meio de balanço de energia e dados de temperatura de uma estação climatológica. Métodos estatísticos de acurácia e similaridade foram usados para validar os resultados. O estudo apresenta uma importante aplicação de sensoriamento remoto para monitorar variáveis hidrometeorológicas em escala espacial na bacia do Rio Pirapó, oferecendo uma alternativa a dados pontuais obtidos por estações terrestres. A malha gerada apresentou ótima correlação, boa similaridade entre os dados de precipitação e evapotranspiração, com baixos erros e incertezas, comprovando a acurácia dos dados espacializados. A malha ajustada pode ser utilizada para a correlação com outros parâmetros hidrometeorológicos, bem como análise espacial das variáveis envolvidas no gerenciamento dos recursos hídricos e no ciclo hidrológico. A metodologia proposta pode aprimorar a gestão dos recursos hídricos, fornecendo dados mais detalhados para previsões de impacto ambiental e gestão sustentável dos meios naturais e antrópicos.

PALAVRAS-CHAVE: Variáveis hidrometeorológicas. Produtos IMERG. Produtos GLDAS.

Spatialization through a rainfall and evapotranspiration data mesh in the Pirapó River sub-basin using remote sensing

ABSTRACT

This work aims to use remote sensing data from the IMERG and GLDAS products based on an average monthly grid of precipitation and evapotranspiration to generate a spatial analysis of the precipitation and evapotranspiration variables in the Pirapó River sub-basin, focusing on the water intake station in Maringá, Paraná, aiming to improve the monitoring and management of water resources. A quantitative approach was applied using a 07x09 cell mesh (100 km² per cell) to map environmental variables from 2000 to 2020. Precipitation was analyzed using Thiessen polygons with data from five rain gauge stations, and evapotranspiration was obtained through energy balance and temperature data from a climatological station. Statistical methods of accuracy and similarity were used to validate the results. The study presents an important application of remote sensing to monitor hydrometeorological variables at a spatial scale in the Pirapó River basin, offering an alternative to point data obtained from ground stations. The generated mesh showed great correlation and good similarity between the precipitation and evapotranspiration data, with low errors and uncertainties, confirming the accuracy of the spatialized data. The adjusted mesh can be used for correlation with other hydrometeorological parameters, as well as for spatial analysis of the variables involved in the management of water resources and the hydrological cycle. The proposed methodology can enhance water resource management by providing more detailed data for environmental impact predictions and sustainable management of natural and anthropogenic environments.

PALAVRAS-CHAVE: Hydrometeorological variables. IMERG products. GLDAS products.

Espacialización mediante una malla de datos de precipitación y evapotranspiración en la subcuenca del río Pirapó utilizando sensores remotos

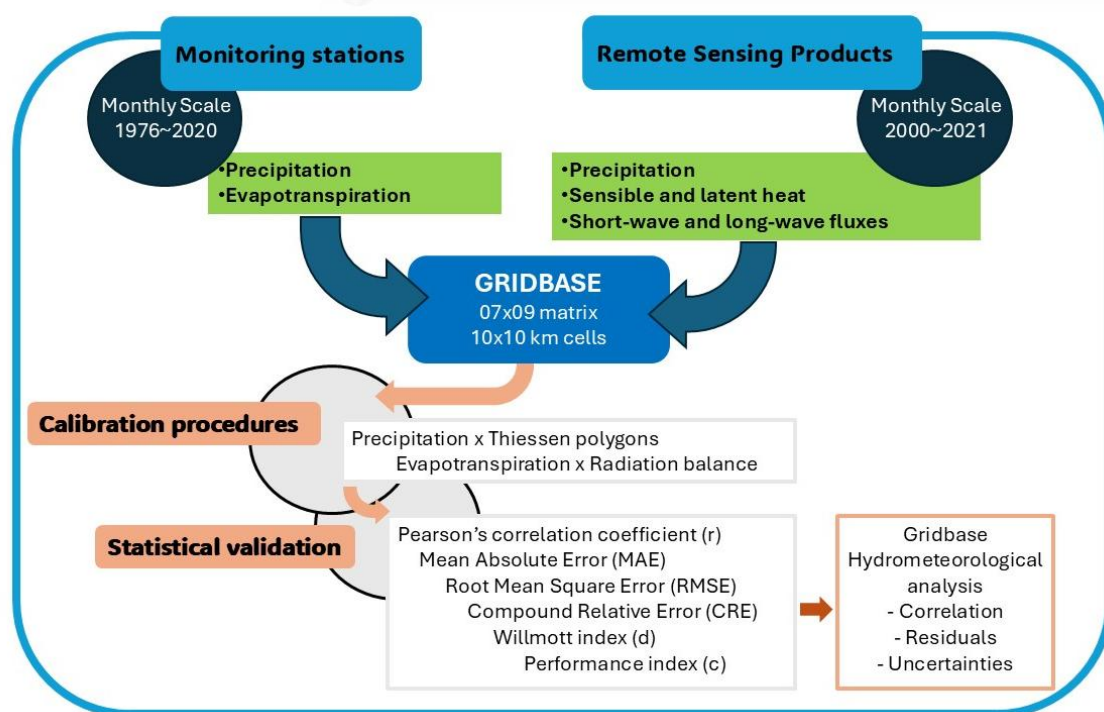
RESUMEN

El presente trabajo tiene como objetivo utilizar datos de sensores remotos de los productos IMERG y GLDAS a partir de una malla de precipitación y evapotranspiración mensual promedio para generar un análisis espacializado de las variables de precipitación y evapotranspiración en la subcuenca del río Pirapó, con exutorio en la estación de captación de agua de Maringá, Paraná, buscando la mejora en el monitoreo y la gestión de los recursos hídricos. Se aplicó un enfoque cuantitativo utilizando una malla de 07x09 celdas (100 km² por celda) para mapear las variables ambientales

de 2000 a 2020. La precipitación se analizó mediante polígonos de Thiessen con datos de cinco estaciones pluviométricas, y la evapotranspiración se obtuvo mediante balance energético y datos de temperatura de una estación climatológica. Se emplearon métodos estadísticos de precisión y similitud para validar los resultados. El estudio presenta una importante aplicación de sensores remotos para monitorear variables hidrometeorológicas a escala espacial en la cuenca del río Pirapó, ofreciendo una alternativa a los datos puntuales obtenidos por estaciones terrestres. La malla generada presentó una excelente correlación, buena similitud entre los datos de precipitación y evapotranspiración, con bajos errores e incertidumbres, comprobando la precisión de los datos espacializados. La malla ajustada puede ser utilizada para la correlación con otros parámetros hidrometeorológicos, así como para el análisis espacial de las variables involucradas en la gestión de los recursos hídricos y en el ciclo hidrológico. La metodología propuesta puede mejorar la gestión de los recursos hídricos, proporcionando datos más detallados para predicciones de impacto ambiental y la gestión sostenible de los medios naturales y antrópicos.

PALABRAS CLAVE: Variables hidrometeorológicas. Productos IMERG. Productos GLDAS.

GRAPHICAL ABSTRACT



1 INTRODUCTION

Studies on climate change and extreme hydroclimatic events have been a focal point in recent decades due to their increasing magnitude and frequency (BHUNYA *et al.*, 2020). From this perspective, data such as precipitation, temperature, and evapotranspiration are essential for analyzing the hydroclimatic patterns of an area or watershed (GOMES *et al.*, 2022). However, land-based monitoring of hydroclimatic variables in smaller areas, such as a drainage area within a Level 3 or higher (Otto Pfafstetter-basin code system), is often flawed and discontinuous. Large areas are frequently represented by a single monitoring point, whether by a climatological or rainfall station, or through surveys conducted in the region.

The goal of hydrometeorological monitoring is to build a database of hydrometric measurements of a watershed for monitoring water quantity and quality-related parameters in different subsystems of the hydrologic cycle (SREPARVATHY; SRINIVAS, 2020). It provides information related to water resources and hydrological variables, which can serve as indicators for analyzing climate change and extreme events in the basin. Such data are crucial for designing sustainable water management strategies and for supporting decision-making in territorial and water resource management projects (POZZONI; SALVETTI; CANNATA, 2020).

Measurements taken by stations (pluviometric, fluviometric, and climatological) are part of the most traditional system within a data collection and monitoring network, providing periodic data measurements for meteorological and hydrological forecasts or other specific purposes (NJUE, 2019). These stations may be conventional, equipped with devices installed at a suitable location, and manual readings by qualified personnel who record and store the data locally; automatic, using sensors programmed to collect data, providing faster response times and direct transfer to a station; and telemetric, following the principles of automatic stations but storing and providing real-time data via a network (OŚRÓDKA; OTOP; SZTURC, 2022; WMO, 2023).

However, such monitoring often generates point data at the fixed location of the station, which does not necessarily represent the full intensity of hydroclimatic parameters in the surrounding area. Therefore, it is necessary to spatialize monitored data using interpolation methods to obtain continuous data across the geographic surface being analyzed (FRANCO; UDA, 2015; WANG *et al.*, 2024).

Geoprocessing and Geographic Information Systems (GIS) can be used to obtain more spatialized hydrometeorological monitoring data for a given area (BRUBACHER *et al.*, 2020). With imaging sensors (satellite images), data collection can occur for a specific area and period, according to the spatial and temporal resolution of the sensor. Satellites monitor extensive regions and various variables (topography, slope, evapotranspiration, vegetation, etc.), providing spatialized data for analyzed parameters (RADOČAJ *et al.*, 2020).

However, care must be taken with the spatial resolution of these images. Higher resolution values result in less detail since the data in each pixel reflects predominant conditions, potentially suppressing finer details not observable at that resolution (CARMO; AZEVEDO; MATIAS, 2023; SILVA *et al.*, 2024).

IMERG (Integrated Multi-satellite Retrievals for GPM) products are the result of precipitation estimates from the GPM (Global Precipitation Measurement) satellite, which has

collected global precipitation data since 2014. Recent IMERG products merge data previously monitored by the TRMM (Tropical Rainfall Measuring Mission) sensor, launched in 1997 by NASA (National Aeronautics and Space Administration) in collaboration with the Japan Aerospace Exploration Agency, and operational from 2000 to 2015. These products provide precipitation monitoring and forecasting images for tropical and subtropical zones, considering interactions between climate and precipitation with air masses and land, also the extensive maritime areas and their influences (BLUMENFELD, 2020; JUNQUEIRA *et al.*, 2022).

Another product for analyzing hydroclimatic parameters via remote sensing is GLDAS (Global Land Data Assimilation System), developed by NASA in partnership with NOAA (National Oceanic and Atmospheric Administration). GLDAS uses a new generation of observation system based on terrestrial and satellite data to integrate the land surface model with meteorological and atmospheric data, providing high-quality global data that represents the Earth's surface conditions, as well as its heat exchanges, and radiation fluxes (RODELL *et al.*, 2004). Through these variables, data on temperature, air humidity, evapotranspiration, and other hydrological parameters can be obtained for specific areas on a monthly, daily, or three-hourly basis.

Proper monitoring of hydroclimatic parameters with greater detail is essential for managing water resources in a certain region. Continuous analysis of water use in sub-basins is required to understand potential changes caused by natural and anthropogenic environments in the hydrological cycle and water resources within the sub-basin.

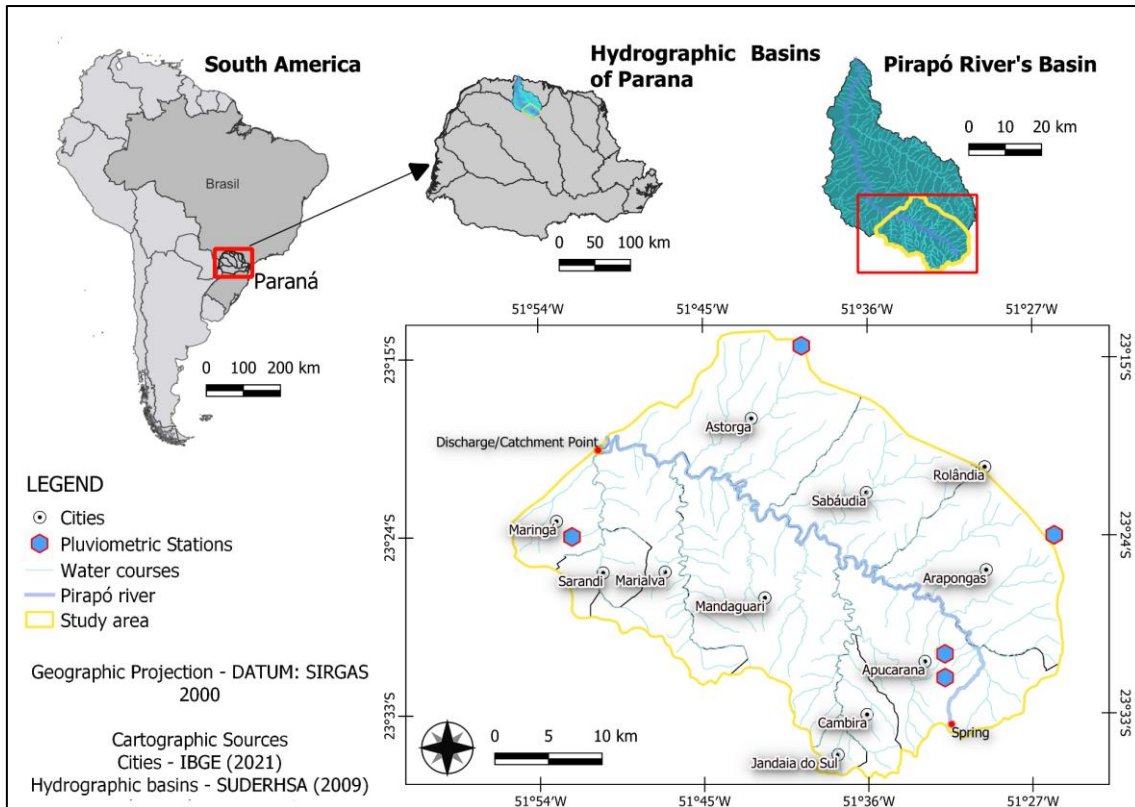
The city of Maringá, located in northern Paraná, uses at least 85% of surface water from the Pirapó River for its urban water supply (CÂMARA MUNICIPAL DE MARINGÁ, 2018), with a sub-basin area of 1,232.40 km² that includes eleven municipalities. Of these, only four cities have rainfall monitoring stations, and there is only one climatological station across the entire region.

Thus, conducting more spatialized hydrometeorological studies to better distribute hydrological cycle variables across the sub-basin is vital for enabling sustainable water resource management. This study aimed to utilize IMERG and GLDAS products from monthly average precipitation and evapotranspiration grids (2000–2020) for the Pirapó River sub-basin, focusing on the water intake station in Maringá, Paraná, as a methodology to obtain spatialized data for the analyzed variables.

2 METHODOLOGY

The study area of this work is the Pirapó River sub-basin, with its source in the Apucarana region, at the geographical coordinates 23°33'33''S; 51°31'27''W, and its mouth at the coordinates 23°19'33''S; 51°50'42''W, at the surface water intake station for the urban water supply of the municipality of Maringá, as shown in Figure 1 (ANA, 2022).

Figure 1 - Study area (sub-basin contributing to the water supply of Maringá)



The predominant characteristic climate of the region is humid subtropical according to the Köppen classification (1978), type Cfa. The characteristics of this climate are warmer, rainier summers, winters without frequent frosts, and no defined dry season. The annual minimum temperature ranges from 15 to 17°C, the maximum annual temperature from 25 to 29°C, and the annual average temperature from 20 to 23°C. The annual average precipitation in the region ranges from 1400 to 1800 mm, with relative humidity of the air between 70 and 75%, and potential evapotranspiration (PET) ranging from 900.1 to 1100 mm (IAPAR, 2019).

For this analysis, the five rainfall stations located in the basin area were considered, where monthly and annual precipitation data were obtained, as well as data from the climatological station of the National Institute of Meteorology of Brazil (INMET), in the municipality of Maringá, where maximum and minimum temperature, actual and potential evapotranspiration data were obtained on a monthly scale. The data from all stations can be seen in Table 1.

Table 1 - Monitoring stations in the area of interest

Station	Station code	Name	Type	Temporal scale	City	Latitude	Longitude	Altitude (m)
P1	2351008	Apucarana (Ubatuba Farm)	Pluviometric ^a	Jan/1976-Sep/1999	Apucarana	-23,500	-51,533	746
P2	2351080	PCH Apucarantina Upstream 2	Pluviometric ^a	Oct/199-Dec/2020	Apucarana	-23,518	-51,530	792
P3	2351048	Arapongas	Pluviometric ^a	Jan/1976-Dec/2019	Arapongas	-23,400	-51,433	793
P4	2351051	Astorga	Pluviometric ^a	Jan/1976-Dec/2019	Astorga	-23,237	-51,661	572
P5	2351045	Guaiapó	Pluviometric ^a	Jan/1976-Dec/2019	Maringá	-23,400	-51,874	584
C1	83767	Maringá	Climatologica ^b	Jan/1990-Dec/2021	Maringá	-23,400	-51,917	542

Note: Worked data from: a - HidroWeb, ANA (2022) e b – INMET (2022)

2.1 Remote sensing and geoprocessing

For spatializing the hydro-meteorological characteristics of the sub-basin, remote sensing products were used (presented in Table 2), so that, when validated with the stations data from the study area, they could provide a characterization of the analyzed variables, as observed in the research by Xavier, King, and Scanlon (2015) and Xavier *et al.* (2021). The remote sensing products were obtained via GES Disc NASA (2022), a provider for downloads from the EarthData platform of the National Aeronautics and Space Administration (NASA).

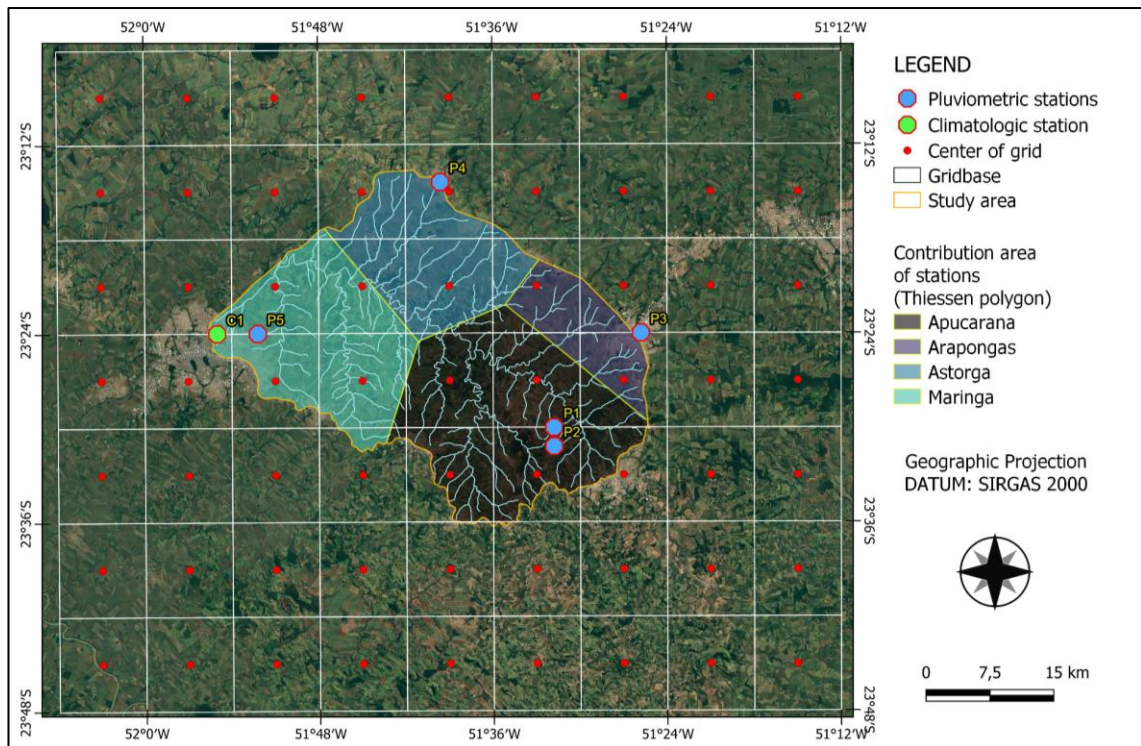
Table 2 - Monthly Scale Remote Sensing Products Obtained from GES DISC NASA

Product	Satellite/Sensor	Spatial resolution	Parameter	Data history	Samples	Flaws
IMERG	GPM/TRMM	10 km	Precipitation (mm h ⁻¹)	Oct/2000-Sep/2021	252	0
GLDAS	NASA	25 km	Sensible and latent heat (W m ⁻²) Short-wave and long-wave fluxes (W m ⁻²)	Jan/2000-Nov/2021	263	0

The IMERG products were used to obtain precipitation data for the study area. GLDAS products were used to obtain actual evapotranspiration, utilizing heat fluxes present in the sub-basin along with the net radiation balance (longwave and shortwave radiation).

Since the spatial resolutions of the remote sensing products obtained had values up to 25 km, the Quantum GIS software (Qgis 3.16.16) was used to delimit a rectangle with boundary geometry of 70 km vertically and 90 km horizontally (coordinates: -52.099; -23.799; -51.199; -23.099). This was done within the Earthdata Search and GES Disc platforms from NASA to retrieve the products determined for analysis. Within this limit, a grid was created (gridbase) in a 07x09 matrix of 10x10 km cells (totaling 70x90 km), which included the smallest spatial resolution range of the sensors used (10 km), with central points that allowed the sampling of data from the raster images (Figure 2).

Figure 2 - Base grid for raster value sampling



Since there is only one climatological station, the parameters obtained from it were considered as the average for the basin with an area of 1,232.40 km². For the rainfall stations in activity, the Voronoi diagram (AURENHAMMER, 1991) was used through the *v.voronoi* function in Qgis software, which generates Thiessen polygons from the centroids of the stations to delimit the area of influence of each station (FORTUNE, 1987).

2.2 Hydrometeorological calibration procedures

Within the grid, each polygon was assigned with values from one to four to establish the influence boundaries of each station: 1 for the Apucarana station, 2 for the Arapongas station, 3 for the Astorga station, and 4 for the Maringá station. The areas of Apucarana (1) and Maringá (4) had the greatest influence, with areas of 472.51 and 351.79 km² respectively, followed by Astorga (3) and Arapongas (2), with areas of 272.25 and 135.86 km², respectively.

For the calibration methodology selection, the work of Xavier, King, and Scanlon (2015) and Xavier *et al.* (2021) were used as a basis, where the arithmetic mean method was the most accurate, with the highest percentage of correct values, considering the seasonality of wet and dry periods. This is because other methods used to spatialize rainfall tend to smooth precipitation, underestimating data in rainy periods and overestimating data in dry periods (0 mm day⁻¹). Thus, the calibration of the data was carried out using the interpolation method, with the arithmetic mean, related to the Thiessen polygons for precipitation, to provide a value for the polygon area overlaid on the grid (which can cover more than one polygon simultaneously due to the spatial resolution of 10 km).

For the calculation and subsequent interpolation of actual evapotranspiration, the

radiation balance in the study area was first analyzed using Equation 1 from the FAO 56 Energy Balance: Crop ET by Allen *et al.* (1998).

$$R_n - G - LE - H = 0 \quad \text{Equação 1}$$

Where, G is the soil heat flux ($W m^{-2}$), H is the sensible heat flux ($W m^{-2}$), LE is the latent heat flux ($W m^{-2}$) e R_n is the net radiation ($W m^{-2}$), given by the difference between the short-wave radiation net balance ($W m^{-2}$) and the longwave radiation net balance ($W m^{-2}$).

By rearranging the equation, the soil heat flux in the study area was determined. Since latent heat flux is a way of expressing evapotranspiration in terms of energy, it was possible to calculate the evapotranspiration in the area using Equation 2.

$$ET = \frac{LE}{L \cdot \rho} = \frac{LE}{(2501 - 2,37T_s) \cdot \rho} \quad \text{Equação 2}$$

Where, L is the latent heat of vaporization in $kJ Kg^{-1}$, T_s is the air temperature at the water surface in $^{\circ}C$, and ρ is the water density in $Kg m^{-3}$. The data used was on a monthly scale, with actual evapotranspiration (ET) reported in $mm month^{-1}$.

2.3 Statistical validation of data

Since interpolations and calibrations were necessary to obtain the historical series derived from remote sensors, the statistical analyses presented in similar research by Xavier, King, and Scalon (2015), and demonstrated by Naghettini and Pinto (2007), were used to assess the accuracy of the acquired data. For this purpose, the following were used: Pearson's correlation coefficient (r), Mean Absolute Error (MAE), Root Mean Square Error (RMSE), and Compound Relative Error (CRE).

In addition, the Willmott index (d) was used to analyze the accuracy of the obtained data in relation to the observed data (WILLMOTT *et al.*, 1985), and the performance index (c) presented by Camargo and Sentelhas (1997), which refers to the reliability of the acquired data.

3 RESULTS AND DISCUSSION

Using IMERG, it was possible to spatialize the data in a way that did not concentrate on a single rainfall station point, since in extreme events, peak values are assigned to the location of the station, and not necessarily to its entire polygon area. Thus, using 20 years of monthly data collected by the GPM and TRMM satellites/sensors, and using the average values found within the defined Thiessen polygons, the graphs in Figures 3 and 4 were obtained, where all months with data gaps from the observed rainfall stations were excluded, and therefore, 190 precipitation data points were examined. Additionally, Table 3 presents the result of the statistical analysis conducted to validate the approximation of satellite-acquired data and remotely sensed observed data.

Figure 3 - Comparison of precipitation data acquired (IMERG) and observed (Station) - (a) Polygon of the Apucarana station (Ap) and (b) Polygon of the Arapongás station (Ar)

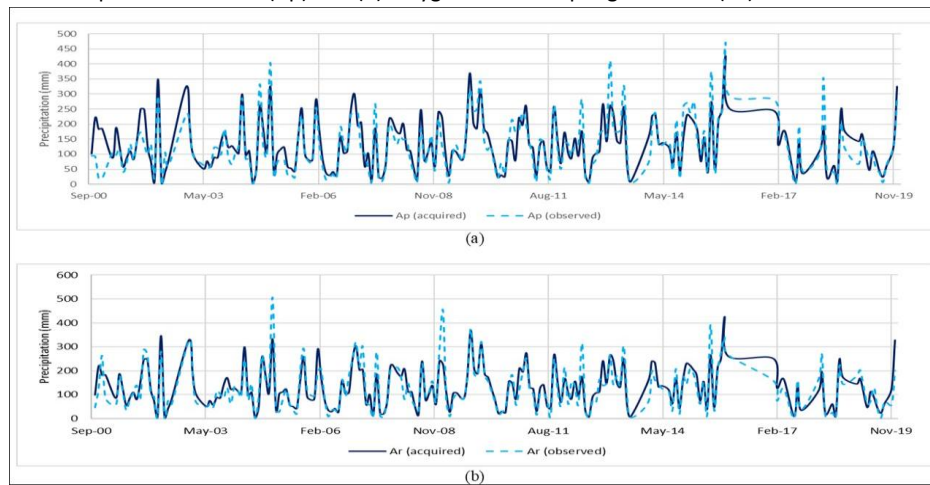


Figure 4 – Comparisons of precipitation data acquired (IMERG) and observed data (Station) - (a) Polygon of the Astorga station (As) and (b) Polygon of the Maringá station (Mg)

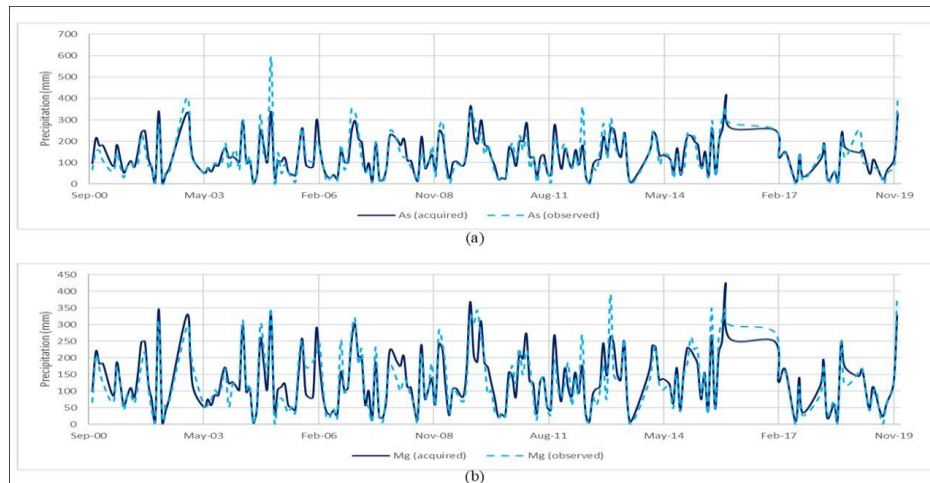


Table 3 – Measures for validation of the average precipitation polygons obtained

Validations	MAE	RMSE	r (Pearson)	CRE	d (Willmott)	c
Apucarana	33.43	46.34	0.87	0.30	0.93	0.81
Arapongas	31.37	46.06	0.88	0.29	0.93	0.81
Astorga	28.73	42.36	0.90	0.25	0.94	0.86
Maringá	28.00	38.62	0.91	0.21	0.95	0.87

In the graphs shown in Figures 3 and 4, the proximity between acquired and observed data can be seen, with moments of underestimation and others of overestimation. These variations are caused by seasonality, the positioning of monitoring points, and the smoothing of precipitation (due to interpolation during spatialization) within the polygon.

Generally, during extreme maximum precipitation events, observed peak values tend to be underestimated. This occurs because such peaks are concentrated at the station, whereas by remote sensing there is an average of the entire area of influence, justifying the underestimation, since in a 10x10 km cell, local detail and variability within the cell are lost.

Conversely, during localized drought periods at the station, the opposite occurs, in which the cell's value is overestimated due to the drag of the average by the precipitation values within the 100 km² area (1 cell).

The values presented in Table 3 show a strong correlation between the data, as evidenced by the Pearson coefficient, along with the good similarity indicated by the CRE. Accuracy measures are also satisfactory, considering the range of values observed. Furthermore, the data exhibit excellent accuracy as indicated by the Willmott index and the confidence/performance index (c).

Unlike the research conducted by Xavier, King, and Scanlon (2015), both the accuracy and similarity of values obtained via remote sensing and observed at the stations demonstrate good performance. This is attributed to the longer temporal scale used in this study (monthly, compared to daily in the authors' research), which reduces potential errors and uncertainties in the acquired data.

To provide a visual analysis of their correlation, scatter plots were generated for precipitation data acquired from remote sensing products and observed (rain gauge stations), as well as for the uncertainties between them, as shown in Figures 5 and 6.

Figure 5 - Scatter plot between acquired and observed precipitation data (in mm) for the polygons: (a) Apucarana, (b) Arapongas, (c) Astorga, and (d) Maringá

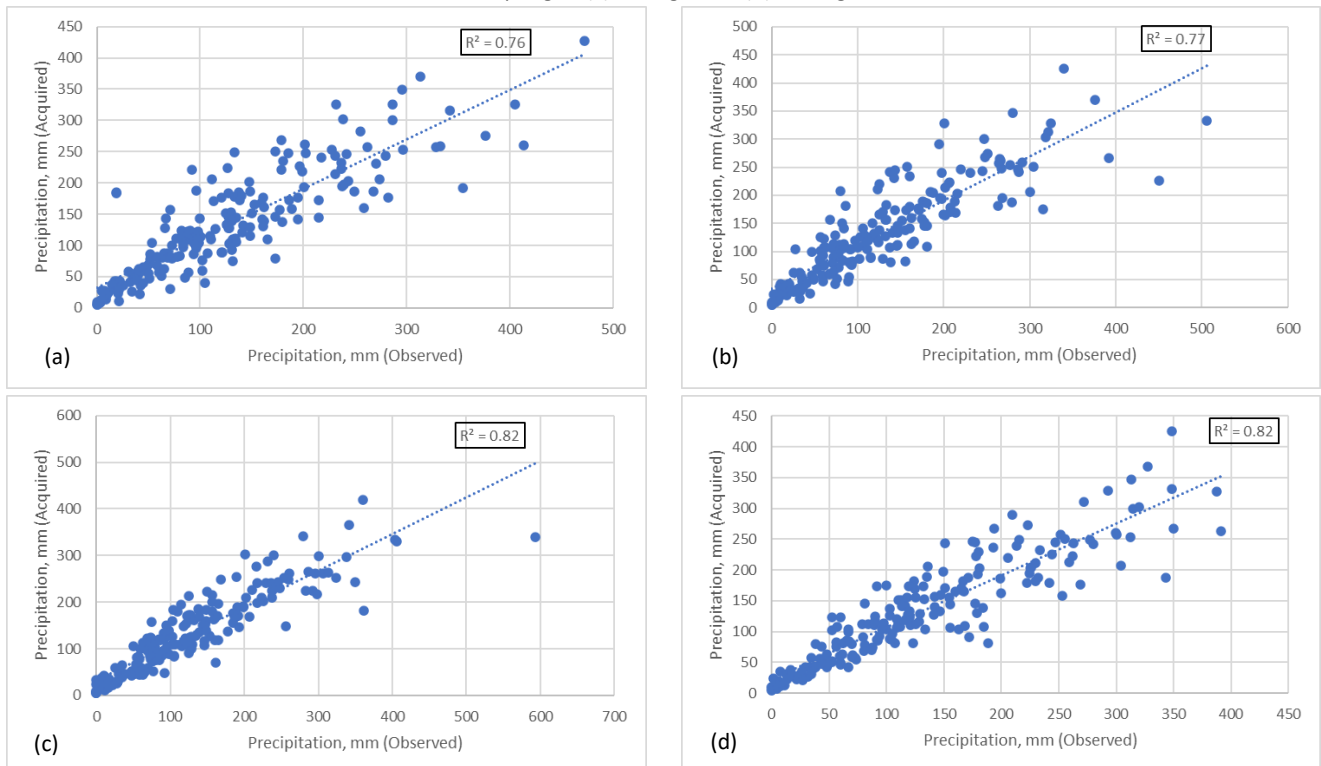
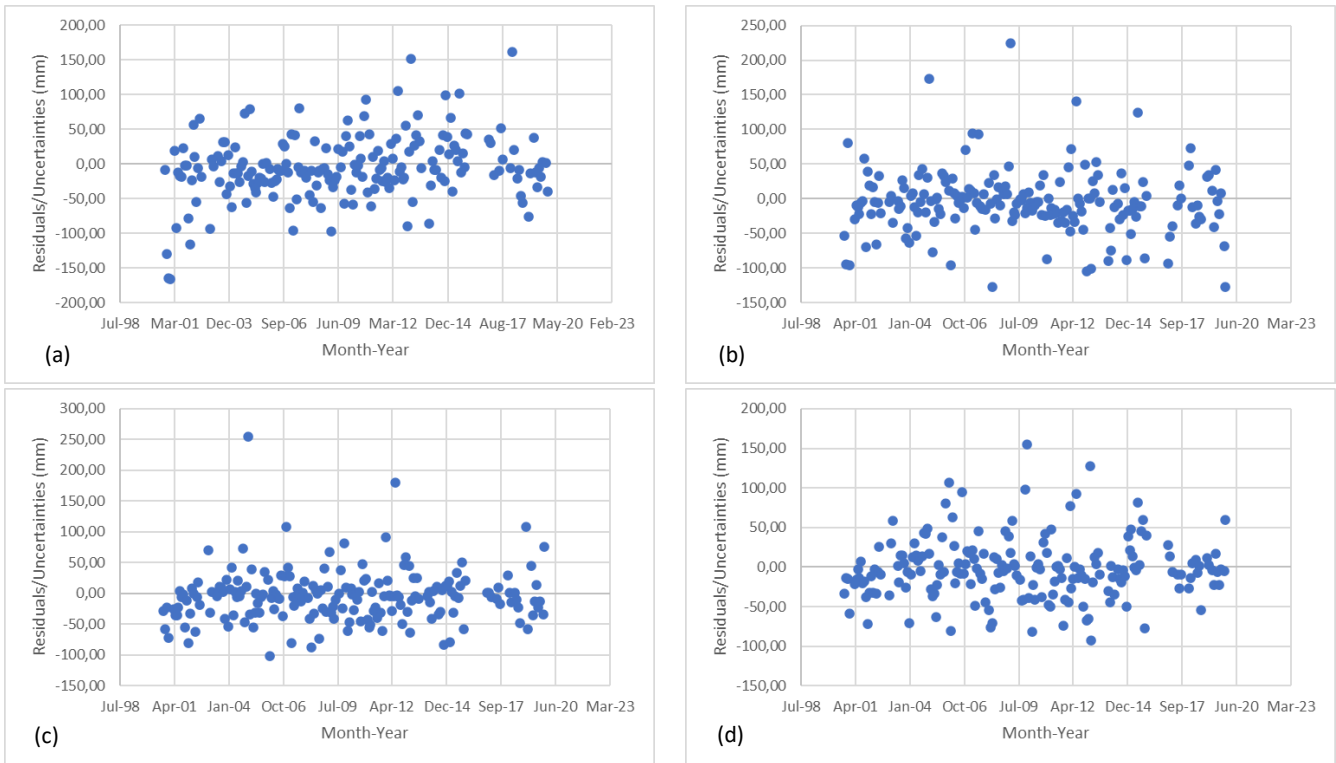


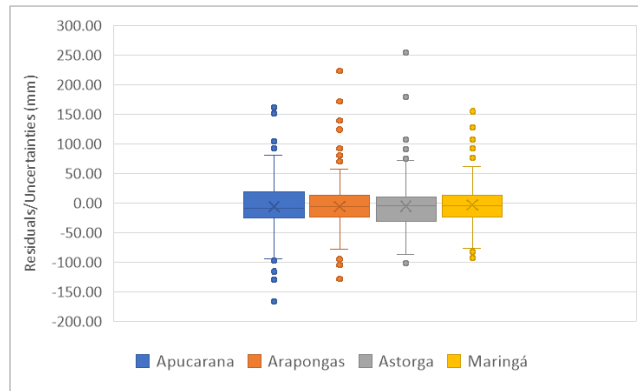
Figure 6 - Scatter plot of residuals/uncertainties over time: (a) Apucarana Station, (b) Arapongas Station, (c) Astorga Station, and (d) Maringá Station



As shown in Figure 5, the observed data for all stations exhibit a linear relationship with the acquired data, although without constant variance, as the values deviate further as precipitation levels increase. This can be attributed to the fact that extreme maximum precipitation values occur specifically at the stations. According to Barni *et al.* (2020), this could result from natural variations in precipitation probabilities or even due to the randomness of rain events. As these events are not necessarily evenly distributed, as by remote sensing data, when the average of the Thiessen polygon that represents the station is considered, leads to a greater dispersion.

Regarding the uncertainties shown in Figure 6, a higher frequency of negative values can be observed, indicating an overestimation of values. However, over time, the uncertainties fluctuated around zero without showing a trend of increase or decrease, and with approximately constant variance. In the Astorga polygon, this frequency is more pronounced, while it is more subtle in Maringá and Apucarana. When presented as a box plot (Figure 7), the predominance of overestimated values and the fluctuation around zero become evident. Additionally, the stations' outliers are highlighted, representing extreme precipitation values—both minimum and maximum—which deviate from the specific values recorded at the stations when spatialized. A similar situation was reported by Barni *et al.* (2020), where the precipitation values obtained via the TRMM satellite showed an attenuation compared to station data due to satellite adjustments and the distributed products. These adjustments resulted in reduced errors and values closer to station averages, allowing for fluctuation around zero.

Figure 7 - Box plot diagram of residuals generated between remotely sensed data and observed data at the pluviometric stations



Using the 22-year average of heat flux in the sub-basin, it was possible to determine the radiation balance in the area through the energy balance, as well as the heat flux components of the balance, as shown in Figures 8 and 9.

Figure 8 - Global radiation balance over 22 years in the sub-basin of interest

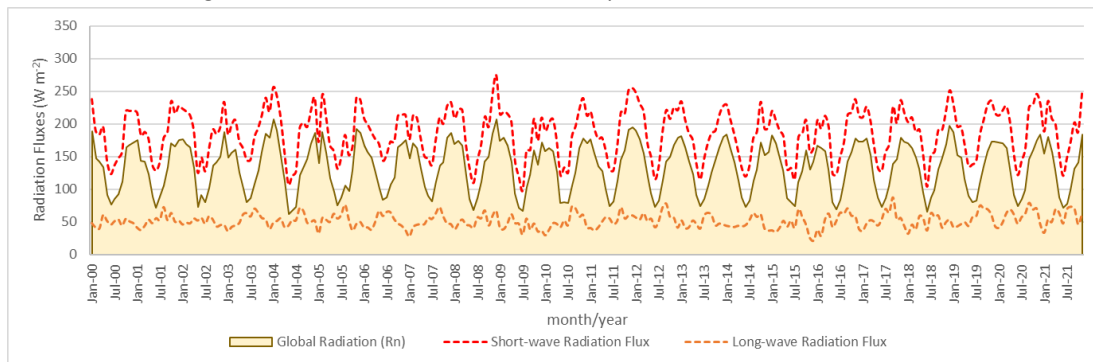
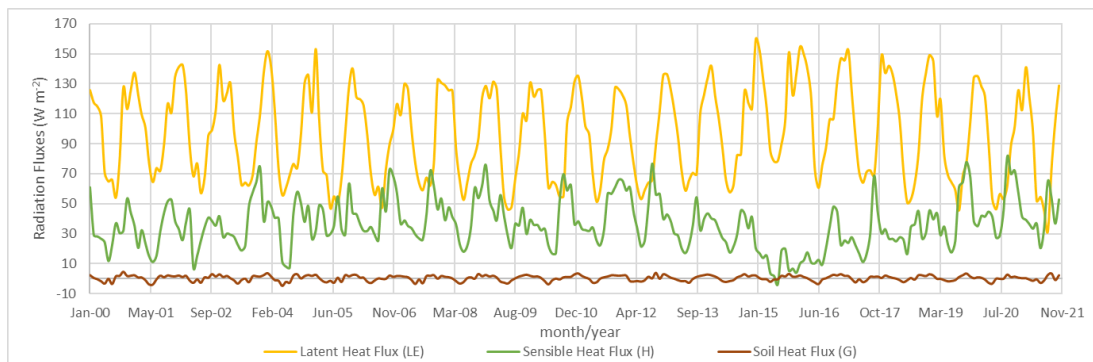


Figure 9 - Components of the global radiation balance (Rn) over 22 years in the sub-basin of interest



It can be seen in Figure 9 that most of the radiation balance in the area comes from the latent heat flux (*LE*), which acts in an upward direction, converting global energy into evapotranspiration from the soil to the atmosphere, as presented in the work of Guauque-Mellado *et al.* (2022).

The soil heat flux acts in a downward direction, entering the soil, representing a small portion of the total radiation balance compared to the other simultaneous heat fluxes. This flux follows a pattern with smaller amplitudes/variations, with minimum extremes reaching negative values, indicating a shift in the flux from downward to upward. In this sense, with low sensible heat and high evapotranspiration, the soil also begins to emit heat during these events.

During periods of water stress, the sensible heat flux tends to be inversely proportional to the latent heat flux, as shown by Vourlitis *et al.* (2008), Biudes *et al.* (2015), and Marques *et al.* (2020). At these times, evapotranspiration increases due to the higher release of latent heat, leading vegetation to reduce water loss. When soil and vegetation moisture levels are optimal, the sensible and latent heat fluxes are proportional, with peaks and valleys showing the loss and recovery of water to the atmosphere. These variations are similar to those observed by Rocha *et al.* (2004), despite the differences in the temporal scales analyzed.

With an average air temperature of 23.37°C, the values of water density from Potter, Wiggert, and Ramadan (2016) were adopted, which is 997 kg m⁻³ at a temperature of 25°C. Thus, using Equation 2, actual evapotranspiration in the sub-basin was obtained, as shown in Figure 10. Using the study area's average temperature and water density for data validation, the Mean Absolute Error (MAE), Root Mean Square Error (RMSE), Pearson's correlation coefficient (r), and Compound Relative Error (CRE) were calculated (Table 4). Scatter plots were also generated for the data and the residuals generated over time (Figure 11).

Figure 10 - Comparison of evapotranspiration values obtained and calculated from the latent heat flux

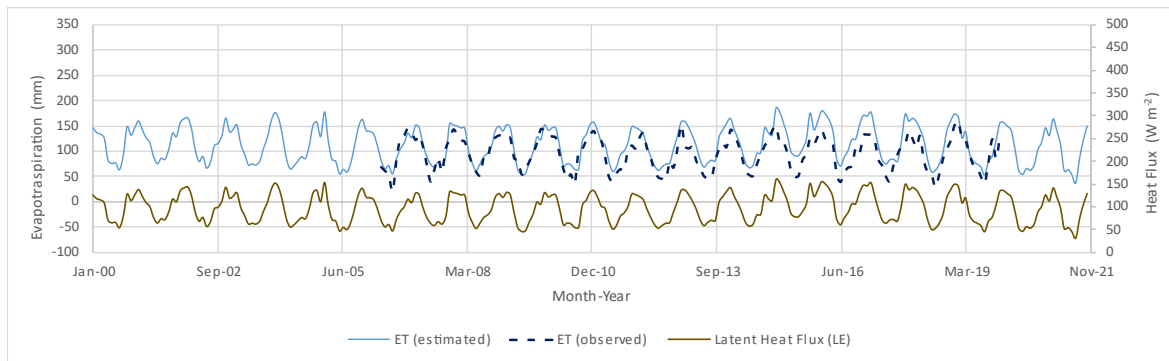


Table 4 - Measures for validation of the obtained Evapotranspiration

Validation	MAE	RMSE	r (Pearson)	CRE	D (Willmott)	c
ETr	15.58	19.33	0.87	0.35	0.9994	0.87

Figure 11 - (a) Scatter plot between the observed values at the climatological station and those acquired through remote sensing, and (b) Dispersion of the residuals generated over time

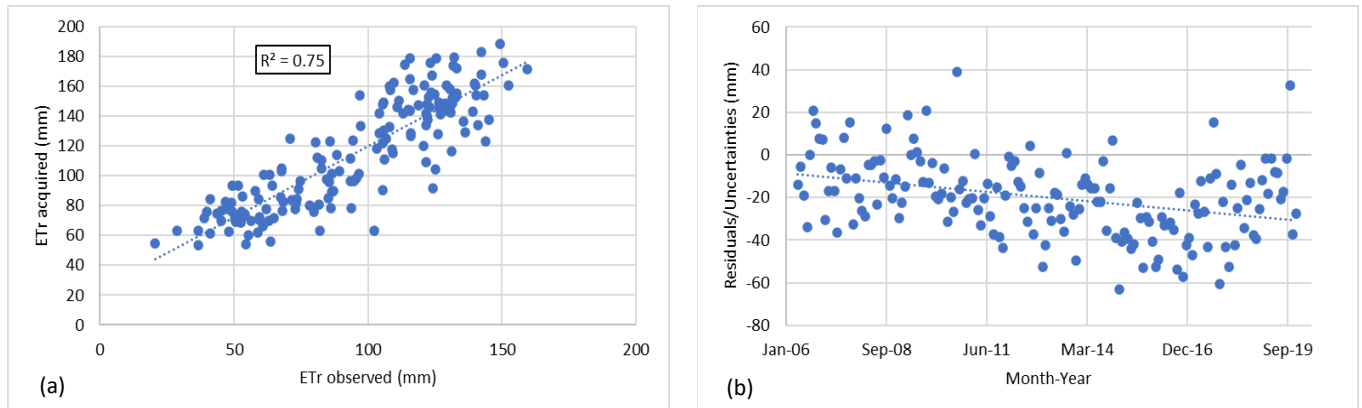


Figure 10 shows that, between 2005 and 2010, the values estimated through remote sensing, adjusted with the average temperature of the sub-basin, exhibit a more symmetrical behavior with the observed values. However, from 2011 to 2018, the values obtained through remote sensing are underestimated in relation to the actual values, even after calibration, suggesting an increase in actual evapotranspiration in the study area.

Considering the total area of 1232.40 km², land use and land cover directly influence evapotranspiration values. In agricultural areas, evapotranspiration drops during periods without vegetation cover, while in forested areas, the fluxes are more constant throughout the year. However, a 100 km² cell in remote sensing does not allow this level of detail, leading to a smoothing of the average relative to the station's point values.

Furthermore, analyzing the results presented in Table 4, it can be concluded that the data show a strong correlation and some similarity, since the CRE does not deviate much from zero. Regarding the accuracy measures, considering a range of more than 100 mm for both the acquired and observed values, both the MAE and RMSE showed low values, indicating good accuracy between the data. The values for the accuracy and confidence index were statistically excellent.

In the scatter plot presented in Figure 11(a), it is evident that the values show a linear relationship, with a satisfactory coefficient of determination ($R^2 > 0.7$), though the variance between the data is not constant. Regarding the uncertainties involved, it can be observed from the data presented in Figure 11(b) that these uncertainties show a negative trend, instead of fluctuating around zero, indicating a greater deviation in evapotranspiration values, with an overestimation of the data, which reflects the land use parameter and the size of the analyzed grid cells. Additionally, it is important to note that the observed data at the climatological station show a time series with a high degree of missing data and a lack of continuity, which may hinder the analysis and comparison of the data.

With the products properly analyzed and statistically validated, the spatialization of the data in the grid base of the study area can be observed in the examples presented in Figures 12 and 13.

Figure 12 - Example of data obtained and processed from the IMERG product for monthly precipitation from 2000 to 2021 in the study area

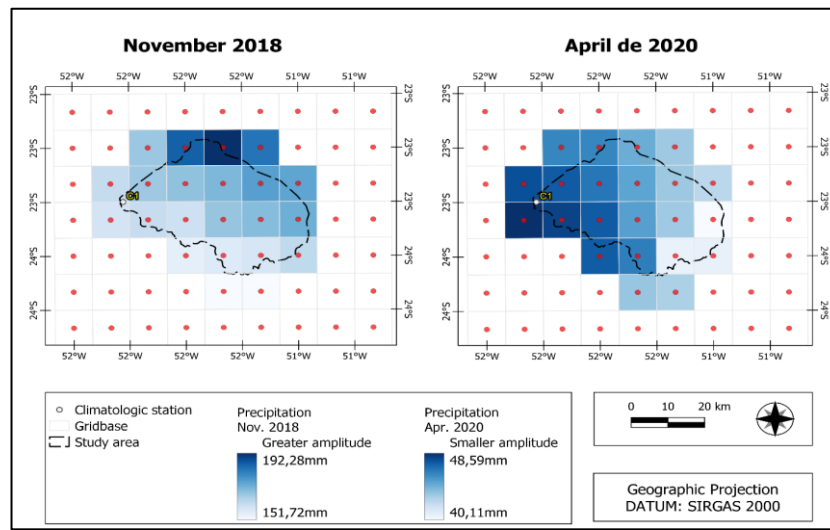
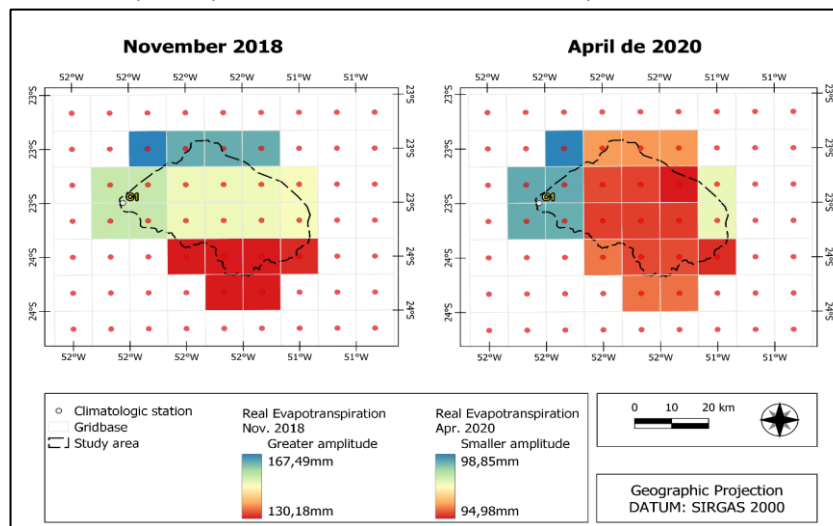


Figure 13 - Example of data obtained and processed from the GLDAS product for monthly actual evapotranspiration from 2000 to 2021 in the study area



In both figures (12 and 13), the data amplitudes obtained in the study area were analyzed according to the gridbase cells, selecting the months with the lowest (November 2018) and highest amplitude (April 2020) for the evapotranspiration variable, which exhibited higher spatial resolution and low variations in the 10 km cells (caused by calibration with local temperature). Considering the number of terrestrial monitoring points, the spatialization proved effective, enabling a gradual analysis of the studied variables and providing a greater amount of data that can be used for water resource management in the region.

4 FINAL CONSIDERATIONS

Thus, this study concludes that considering the need for spatialized hydrometeorological variables, the use of remote sensing data effectively enabled the

adjustment of a hydrometeorological parameter grid in the study area, allowing for more detailed analysis of the sub-basin.

This approach allows for future expansion to other areas and, when combined with a broader range of observed data from monitoring stations, could significantly improve data accuracy. Furthermore, correlating these data with hydrological cycle variables obtained at lower spatial resolutions from other remote sensing products would refine the acquired data, offering greater variability gradients and detailed insights into study areas, particularly pre-delineated sub-basins.

For a more significant test, one option would be to conduct in situ monitoring of certain hydrological cycle variables that are critical for determining specific components of the basin, as well as the water resource systems from the area, which could be used for calibrating remote sensing products.

Understanding uncertainties within hydrometeorological processes, as well as their assessment in water resource management, is essential for generating environmental products and models that closely represent environmental phenomena and provide reliable data for analyzing and predicting factors that may impact natural and anthropogenic systems.

5 REFERENCES

ALLEN, R. G., *et al.* Crop evapotranspiration-Guidelines for computing crop water requirements-FAO Irrigation and drainage paper 56. **Food and Agriculture Organization of the United Nations (FAO), Rome**, v. 300, n. 9, p. D05109, 1998.

ANA - AGÊNCIA NACIONAL DE ÁGUAS. **HidroWeb**: sistemas de informações hidrológicas. 2022. Disponível em: <<http://hidroweb.ana.gov.br/>>. Acesso em: 20 mar. 2022.

AURENHAMMER, F. *Voronoi Diagrams - A Survey of a Fundamental Geometric Data Structure*. **ACM Computing Surveys**, v. 23, n. 3, p. 345-405, 1991.

BARNI, P. E. *et al.* Precipitação no extremo norte da Amazônia: distribuição espacial no estado de Roraima, Brasil. **Sociedade & Natureza**, v. 32, p. 439-456, 2020. <https://doi.org/10.14393/SN-v32-2020-52769>.

BHUNYA, P. K. *et al.* A Review of Case Studies on Climate Change Impact on Hydrologic Cycle: An Indian Perspective. **International Journal of Scientific Research in Science, Engineering and Technology**, v. 7, n. 5, p. 249-266, September-October-2020. <https://doi.org/10.32628/IJSRSET207548>.

BIUDES, M. S. *et al.* Patterns of energy exchange for tropical ecosystems across a climate gradient in Mato Grosso, Brazil. **Agricultural and Forest Meteorology**, v. 202, p. 112-124, 2015. <https://doi.org/10.1016/j.agrformet.2014.12.008>.

BLUMENFELD, J. **From TRMM to GPM: The Evolution of NASA Precipitation Data** | Earthdata, 2020. Disponível em: <<https://www.earthdata.nasa.gov/learn/articles/trmm-to-gpm>>. Acesso em: 28 abr. 2023.

BRUBACHER, J.P.; OLIVEIRA, G.G.; GUASSELLI, L.A. Preenchimento de Falhas e Espacialização de Dados Pluviométricos: Desafios e Perspectivas. **Revista Brasileira de Meteorologia**, v. 35, n. 4, p. 615-629, 2020. <http://dx.doi.org/10.1590/0102-7786354006>.

CÂMARA MUNICIPAL DE MARINGÁ. **Sala de Imprensa - Hiroshi Fukumoto. Guardiã da nascente do Rio Pirapó foi homenageado com Brasão do Município**. Assessoria de Imprensa. 2018. Disponível em: <<https://www.cmm.pr.gov.br/?inc=noticia&id=3493>>. Acesso em: 15 jan. 2023.

CAMARGO, A. P.; SENTELHAS, P.C. Avaliação do desempenho de diferentes métodos de estimativa de evapotranspiração potencial no Estado de São Paulo, Brasil. **Revista Brasileira de Agrometeorologia**, v. 5, n. 1, p. 89-97, 1997.

CARMO, B. A.; AZEVEDO, T.; MATIAS, L. F. As imagens de sensoriamento remoto no planejamento urbano de cidades pequenas: a necessidade da adoção de imagens aéreas. In: XX SIMPÓSIO BRASILEIRO DE SENSORIAMENTO REMOTO. 2023, Florianópolis – SC. *Anais [...]*. Florianópolis – SC.: SBSR, v. 20, 2023.

FORTUNE. S. J. A Sweepline Algorithm for Voronoi Diagrams. **Algorithmica** 2. p. 153-174, 1987.

<https://doi.org/10.1007/BF01840357>.

FRANCO, A. C. L.; UDA, P. K. Comparação de métodos de espacialização da precipitação na bacia do alto rio Negro, Santa Catarina. In: XVII SIMPÓSIO BRASILEIRO DE SENSORIAMENTO REMOTO. 2015, João Pessoa-PB. *Anais [...]*. João Pessoa-PB: INPE, 2015. p. 3052-3058.

GOMES, D. J. C., *et al.* Estimativa de precipitação dos dados CHIRPS e GPCC em anos de extremos climáticos, Bacia Hidrográfica do rio Guamá-PA. **Revista Brasileira de Geografia Física**, v.15, n. 03, p. 1583-1598, 2022.

GUAUQUE-MELLADO, D. *et al.* Evapotranspiration under Drought Conditions: The Case Study of a Seasonally Dry Atlantic Forest. **Atmosphere**, v. 13, n. 6, p. 871, 1 jun. 2022. <https://doi.org/10.3390/atmos13060871>.

IAPAR - Instituto Agrônômico do Paraná (2019) Atlas climáticos do Paraná. Disponível em:

<<https://www.idrparana.pr.gov.br/Pagina/Atlas-Climatico>>. Acesso em 16 jun. 2021.

INMET. Instituto Nacional de Meteorologia (2022) Gráficos. Disponível em:

<<https://portal.inmet.gov.br/servicos/bdmep-dados-hist%C3%B3ricos>>. Acesso em: 20 mar. 2022.

JUNQUEIRA, R. *et al.* Hydrological modeling using remote sensing precipitation data in a Brazilian savanna basin.

Journal of South American Earth Sciences, v. 115, April 2022, 103773.

<https://doi.org/10.1016/j.jsames.2022.103773>.

KÖPPEN. W. Climatologia. México: Fundo de Cultura Econômica, 1978.

MARQUES, T. V. *et al.* Environmental and biophysical controls of evapotranspiration from Seasonally Dry Tropical Forests (Caatinga) in the Brazilian Semi-arid. **Agricultural and Forest Meteorology**, v. 287, 107957, 2020.

<https://doi.org/10.1016/j.agrformet.2020.107957>.

NAGHETTINI. M.; PINTO. E. J. A. Hidrologia Estatística. Belo Horizonte: CPRM, 2007.

NJUE, N. *et al.* Citizen science in hydrological monitoring and ecosystem services management: State of the art and future prospects. **Science of The Total Environment**, v. 693, 133531, 2019.

<https://doi.org/10.1016/j.scitotenv.2019.07.337>.

OŚRÓDKA; K.; OTOPI, I.; SZTURC, J. Automatic quality control of telemetric rain gauge data providing quantitative quality information (RainGaugeQC), **Atmos. Meas. Tech.**, 15, p. 5581-5597. 2022. <https://doi.org/10.5194/amt-15-5581-2022>.

POTTER. M.C. WIGGERT. D.C., RAMADAN, B. **Mecânica dos Fluidos**, 4. ed. São Paulo: Cengage Learning. 2016.

POZZONI, M., SALVETTI, A., CANNATA, M. Retrospective and prospective of hydro-met monitoring system in the Canton Ticino, Switzerland. *Hydrological Sciences Journal*, 67(16), p. 2386-2400, 2020.

<https://doi.org/10.1080/02626667.2020.1760280>.

RADOČAJ, D. *et al.* Global Open Data Remote Sensing Satellite Missions for Land Monitoring and Conservation: A Review. *Land*, 9, 402, 2020. <https://doi.org/10.3390/land9110402>.

ROCHA, H. R. *et al.* Seasonality of water and heat fluxes over a tropical forest in eastern amazonia. **Ecological Applications**, v. 14, n. 4, p. 22-32, 2004.

RODELL, M. *et al.* The Global Land Data Assimilation System. **Bulletin of the American Meteorological Society**, v. 85, n. 3, p. 381-394, 2004. <https://doi.org/10.1175/BAMS-85-3-381>.

SILVA, A. L. P. *et al.* O uso do sensoriamento remoto na biodiversidade e conservação. **Peer Review**, v. 6, n. 7, 2024. Disponível em: <<http://repositorio.ufra.edu.br/jspui/handle/123456789/2235>>. Acesso em: 29 de maio de 2024.

SREEPARVATHY, V., SRINIVAS, V.V. A fuzzy entropy approach for design of hydrometric monitoring networks. **Journal of Hydrology**, v. 586, 124797, 2020. <https://doi.org/10.1016/j.jhydrol.2020.124797>.

VOURLITIS, G. L. *et al.* Energy balance and canopy conductance of a tropical semi-deciduous forest of the southern Amazon Basin. **Water Resources Research**, v. 44, n. 3, mar. 2008. <https://doi.org/10.1029/2006WR005526>.

WANG, Y.; LIU, X.; LIU, R.; ZHANG, Z. Research Progress on Spatiotemporal Interpolation Methods for Meteorological Elements. **Water**, v., 16, n. 6, 818, 2024. <https://doi.org/10.3390/w16060818>.

WILLMOTT, C. J. *et al.* Statistics for the evaluation of model performance. **Journal of Geophysical Research**, v. 90, n. C5, p. 8998-9005, 1985.

WMO - World Meteorological Organization. **Guide to Meteorological Instruments and Methods of Observation**. WMO-No. 8. Geneva: World Meteorological Organization, 2023.

XAVIER, A. C. *et al.* New improved Brazilian daily weather gridded data (1961-2020). **International Journal of Climatology**, n. May, p. 1-15, 2021. <https://doi.org/10.1002/joc.7731>.

XAVIER, A. C.; KING, C. W.; SCANLON, B. R. Daily gridded meteorological variables in Brazil (1980-2013). **International Journal of Climatology**, v. 36, n. 6, p. 2644-2659, 2015. <https://doi.org/10.1002/joc.4518>.

6 DECLARATIONS

6.1 Contribution of each author

Lucas Vinicius Dias: Conceptualization and Study Design, Data Curation, Formal Analyses, Funding Acquisition, Investigation, Methodology, Writing - Original Draft.

Lais Ferrer Amorim de Oliveira: Conceptualization and Study Design, Methodology, Writing - Critical Review, Supervision.

Paulo Fernando Soares: Conceptualization and Study design, Methodology, Writing - Critical Review, Supervision.

Cláudia Telles Benatti: Conceptualization and Study Design, Methodology, Writing - Critical Review, Revision and Final Edition, Supervision.

6.2 Declaration of conflicts of interest

We, Lucas Vinicius Dias, Lais Ferrer Amorim de Oliveira, Paulo Fernando Soares, and Cláudia Telles Benatti, declare that the manuscript titled " Spatialization through a rainfall and evapotranspiration data mesh in the Pirapó River sub-basin using remote sensing":

1. **Financial Ties:** There are no financial ties that could influence the results or interpretation of the work. This study was financed in part by the Coordenação de Aperfeiçoamento de Pessoal de Nível Superior - Brasil (CAPES) - Finance Code 001.



2. **Professional Relationships:** There are no professional relationships that could affect the analysis, interpretation, or presentation of the results.
3. **Personal Conflicts:** There are no personal conflicts of interest related to the content of the manuscript.